Available online at www.sciencedirect.com
SCIENCE DIRECT®
Developmental Biology 266 (2004) 252–269
DEVELOPMENTAL BIOLOGY
www.elsevier.com/locate/ydbio

Combined intrinsic and extrinsic influences pattern cranial neural crest migration and pharyngeal arch morphogenesis in axolotl

Robert Cerny,[a,b,*] Daniel Meulemans,[c] Jürgen Berger,[d] Michaela Wilsch-Bräuninger,[e] Thomas Kurth,[f] Marianne Bronner-Fraser,[c] and Hans-Henning Epperlein[a]

[a] *Department of Anatomy, TU Dresden, Dresden 01307, Germany*
[b] *Department of Zoology, Charles University, Prague 128 44, Czech Republic*
[c] *Division of Biology, 139-74 California Institute of Technology, Pasadena, CA 91125, USA*
[d] *Max-Planck-Institute for Developmental Biology, Tübingen 72076, Germany*
[e] *Max-Planck-Institute for Molecular Cell Biology and Genetics, Dresden 01307, Germany*
[f] *Department of Biology, TU Dresden, Dresden 01062, Germany*

Received for publication 10 May 2003, revised 15 August 2003, accepted 9 September 2003

Abstract

Cranial neural crest cells migrate in a precisely segmented manner to form cranial ganglia, facial skeleton and other derivatives. Here, we investigate the mechanisms underlying this patterning in the axolotl embryo using a combination of tissue culture, molecular markers, scanning electron microscopy and vital dye analysis. In vitro experiments reveal an intrinsic component to segmental migration; neural crest cells from the hindbrain segregate into distinct streams even in the absence of neighboring tissue. In vivo, separation between neural crest streams is further reinforced by tight juxtapositions that arise during early migration between epidermis and neural tube, mesoderm and endoderm. The neural crest streams are dense and compact, with the cells migrating under the epidermis and outside the paraxial and branchial arch mesoderm with which they do not mix. After entering the branchial arches, neural crest cells conduct an "outside-in" movement, which subsequently brings them medially around the arch core such that they gradually ensheath the arch mesoderm in a manner that has been hypothesized but not proven in zebrafish. This study, which represents the most comprehensive analysis of cranial neural crest migratory pathways in any vertebrate, suggests a dual process for patterning the cranial neural crest. Together with an intrinsic tendency to form separate streams, neural crest cells are further constrained into channels by close tissue apposition and sorting out from neighboring tissues.

Keywords: Axolotl; Head; Cranial neural crest; Migration; Branchial arches; AP-2; Snail

Introduction

The neural crest is a transient population of cells that arises from the dorsal neural tube of vertebrate embryos. These cells migrate extensively along defined pathways to give rise to a wide variety of derivatives including pigment cells, neurons and glia (Hall and Hörstadius, 1988; Le Douarin and Kalcheim, 1999). Although both head and trunk neural crest cells share many common derivatives, connective and supportive tissues are predominantly generated by cranial neural crest (Couly et al., 1993; Jiang et al., 2002; Noden, 1988; but see Epperlein et al., 2000; McGonnell and Graham, 2002).

An important question is how cranial neural crest cells are directed to their ultimate destinations during embryogenesis. Fate mapping and transplantation experiments have demonstrated that inherent information in the hindbrain (Lumsden and Krumlauf, 1996; Trainor and Krumlauf, 2000b) contributes to cranial neural crest migratory pattern (Lumsden et al., 1991) and cell fate decisions. However, cell and tissue interactions are also critical (Trainor and Krumlauf, 2000a; Trainor et al., 2002), emphasizing the importance of understanding interactions between neural crest cells and their surrounding environment both at the neural tube and branchial arch level (Farlie et al., 1999; Golding et al., 2002; Trainor et al., 2002).

* Corresponding author. Department of Anatomy, Medizinisch-Theoretisches Zentrum, TU Dresden, Fetscherstrasse 74, 01307 Dresden, Germany. Fax: +49-351-458-6303.
E-mail address: cerny8@natur.cuni.cz (R. Cerny).

0012-1606/$ - see front matter © 2003 Elsevier Inc. All rights reserved.
doi:10.1016/j.ydbio.2003.09.039

Because it is a uniquely vertebrate structure, evolution of the neural crest is intimately interlinked with vertebrate origins (Shimeld and Holland, 2000). To date, neural crest migration is best understood in the avian embryo, though mouse and zebrafish mutants have also improved our understanding of the molecular mechanisms guiding neural crest migration and branchial arch patterning. Much less is known about neural crest migration in other vertebrates. Comparative analysis of neural crest migration in a number of vertebrate species is critical because it can elucidate fundamental vertebrate features as well as reveal mechanisms for generating distinct cranial morphologies. The axolotl possesses several advantages for analyzing pathways of neural crest migration. The slow development of axolotl embryos and their relatively large size allows a gradual tracing of neural crest migration. Furthermore, the premigratory neural crest in axolotl is morphologically distinguishable from the rest of the neural tube, facilitating cell lineage tracing with vital dyes. In the present study, we use the axolotl to investigate whether cranial neural crest migration and patterning into streams is regulated autonomously and/or influenced by adjacent tissues. We identify neural crest cells and the surrounding tissues with a combination of molecular markers, scanning electron microscopy and vital dye analysis in vivo and study cranial neural crest migration from isolated neural tube explants in vitro.

Our results reveal that neural crest cells initially migrate from the neural tube in an autonomous manner, forming separate streams emanating from the hindbrain. Later, these streams are further constrained by ectodermal infoldings that create channels for neural crest migration. At the pharyngeal level, we demonstrate for the first time that cranial neural crest cells migrate initially superficial to the branchial arch mesoderm with which they do not intermix. Then they conduct an ''outside-in'' movement that brings them medial to the arch core and in contact with pharyngeal endoderm. Such a shift in migration is a new developmental mechanism that has been hypothesized in zebrafish (Kimmel et al., 2001) but not previously documented in any vertebrate. The results demonstrate that patterning of the axolotl neural crest involves a combination of intrinsic and extrinsic influences.

Materials and methods

Embryos

Embryos of the Mexican axolotl (*Ambystoma mexicanum*) were obtained, reared and staged as previously described (Epperlein et al., 2000). Before operating on the embryos, they were decapsulated manually.

Injections of DiI and GFP

DiI injection was performed as described previously (Epperlein et al., 2000). For injection, an IM 300 microinjector with fine glass micropipettes that were attached to a needle holder were used (Oxford instruments).

For ectopic expression of GFP (green fluorescent protein) about 1–5 ng GFP mRNA (in 20 nl solution) was injected with a picospritzer into one blastomere of axolotl embryos at a two- to four-cell stage. For injection, the embryos were placed in an agar dish containing 5% Ficoll in normal strength Steinberg solution with antibiotics. After 1 day, the embryos were transferred into 20% saline and after gastrulation into normal strength saline. Embryos were allowed to develop to the neurula stage (15–16) and then used for grafting.

Grafting experiments

Using tungsten needles, green fluorescent head neural fold segments (region 2–7; see Epperlein et al., 2000) from neurulae (stages 16–18) injected with GFP mRNA at the two-cell stage were grafted orthotopically into uninjected hosts (n = 13) and used for the analysis of cranial neural crest migration.

For culturing early cranial neural tubes, the head epidermis was removed from embryos at stages 20–22 (n = 11). Neural tubes reaching from the level of the prosencephalon till the end of the rhombencephalon were carefully excised and placed on a permissive substrate (a polylysine-coated glass disk incubated with fibronectin (100 μg/ml; Sigma). Small pieces of glass were used to press the neural tube against the substrate. Cultures were grown in small plastic dishes at room temperature containing Steinberg solution with antibiotics.

For another experiment, the head epidermis was removed from embryos at stages 23–26 in regions of prospective hyoid and branchial arch neural crest streams. Operations were carried out at room temperature in agar dishes (2% agar in Steinberg solution) containing distilled water and antibiotics. After the operations, embryos were reared in Steinberg solution and allowed to develop to a larval stage.

Histology and immunostaining

Embryos were anaesthetized in a solution of tricaine methane-sulfonate (MS-222, Sandoz) and fixed in 4% paraformaldehyde in 0.1 M phosphate-buffered saline (PFA/PBS) overnight. After washing in PBS, specimens were dehydrated through a graded series of ethanol and embedded in JB4 (Polysciences, Inc.). Sections (5 μm) were cut with a Reichert-Jung microtome (Biocut 2035), stained with Azure B–Eosin (SERVA) and mounted in DePeX (SERVA). Embryos processed through in situ hybridization were stored in 100% methanol and cut (100 μm) using a Vibratome Series 1000 sectioning system (Ted Pella, Inc.). Sections were counterstained with a primary polyclonal anti-fibronectin antibody (1:100, Dako) followed by a goat anti-rabbit Cy3 secondary antibody (1:100, Dako) to visualize tissue borders. Afterwards, these sections were stained with DAPI (0.1–1 μg/ml PBS) to mark cell nuclei.

Whole-mount double-staining of embryos fixed in DMSO/methanol was performed using mouse monoclonal anti-actin antibodies (CLT 9001, Cedarlane) and polyclonal rabbit anti-β-catenin antibodies (P14L; Schneider et al., 1996). These primary antibodies were detected by goat anti-mouse Alexa 488 (1/50, Molecular Probes) and goat anti-rabbit Cy3 (1/500, Dianova). Incubation times for primary and secondary antibodies were 2–3 days at room temperature to allow complete antibody penetration. Following washing in PBS and postfixation in PFA/PBS, specimens were dehydrated and embedded in Technovit 7100 (Kulzer). Sections (3–5 μm) were counterstained with DAPI to visualize cell nuclei.

Cartilage staining

Larvae (13–17 mm long) were anaesthetized with MS-222, fixed in PFA/PBS overnight, rinsed and transferred into 80% ethanol. Cartilage was visualized with alcian blue using a modified protocol of Kimmel et al. (1998). Staining lasted for about 20 h (at room temperature). After destaining in acid–alcohol and rinsing in PBS, specimens were treated for about 15 h with a mixture of trypsin (0.05%) and EDTA (0.02%) in PBS. Then cartilages were dissected free from surrounding tissue, cleared in a mixture of KOH (1%) and H_2O_2 (1%) under intense illumination and transferred to glycerol/ethanol (1:1).

Scanning electron microscopy

For a direct visualization of cranial neural crest streams, the head epidermis was removed from embryos (stages 18–30) prefixed in Karnovsky's fixative using tungsten needles. After rinsing in PBS, embryos were postfixed with 4% osmium tetroxide. Following another rinse, embryos were dehydrated through a graded series of ethanol, critical point-dried (liquid CO_2), sputter-coated with gold-palladium and examined under scanning electron microscopes LEO 430 or Hitachi S-800.

In living embryos at stage 23–24, the cranial epidermis was folded back on the left side to expose the epidermal invaginations at r3 and r5. The operations were carried out in ice-cold Steinberg solution (fourfold strength) using tungsten needles. Operated embryos were processed further for SEM as indicated above.

Apoptosis

Embryos (stages 17–28) were fixed in MEMFA and stored in 100% methanol at −20°C. After gradual rehydration, embryos were labeled using TUNEL (In Situ Cell Death Detection Kit, Roche). For a negative control, the embryos were incubated in the labeling buffer omitting the enzyme component. No phosphatase positive cells were observed under these conditions, indicating that no endogenous phosphatases were labeled in the experimental embryos. For a positive control, chick embryonic limb buds (7–8 days) and *Xenopus* embryos (stages 24–35) were stained. NBT/BCIP was used for a substrate to visualize the alkaline phosphatase signal.

Cell division

Embryos (stages 20–29) were fixed in PFA/PBS and postfixed in DMSO/methanol. After rehydration, embryos were stained with anti-Phosphohistone-3 (1 μg/ml; Upstate Biotechnology; Hendzel et al., 1997; Saka and Smith, 2001) that detects cells at late G2 to telophase. Antibody incubation was performed overnight at room temperature. Bound anti-Phosphohistone-3 was detected with secondary biotinylated antibodies and a tertiary Avidin–Peroxidase complex. DAB was used as a substrate for the peroxidase (Vectastain Elite ABC Kit). To block endogenous peroxidase, embryos were treated with 1% H_2O_2/PBS before antibody incubation. DAB-stained embryos were washed, postfixed in PFA/PBS and dehydrated in a graded series of methanol. The pigment of embryos was bleached in methanol/H_2O_2. Embryos were cleared in a mixture of benzyl alcohol and benzyl-benzoate (1:2). As a negative control, albino embryos processed in parallel but without the antibody incubation displayed no DAB staining (not shown), ensuring that the observed signals are not due to the activity of endogenous peroxidases.

In situ hybridization of AP-2, Snail and Fgf-8

cDNA was synthesized from *Ambystoma* embryo total RNA (stages 22–35) by poly-T-primed reverse transcription and used as a template for PCR. The following degenerate primers were designed against conserved regions of vertebrate Snail genes and used to amplify an approximately 400 bp fragment of the *Ambystoma* Snail homolog; 5′ primer, AAGACCTAYTCYACKTTCTCTGGG, 3′ primer, CAGCARCCAGAYTCCTCATG. The fragment was cloned, sequenced and compared to known Snail genes using the Megalign program. The conceptual translation product of the axolotl *snail*-like PCR fragment is 84% identical to *Xenopus* Snail and 82% identical to *Xenopus* Slug. Due to high conservation in the amplified zinc-finger region, we cannot conclusively assign this gene to either the Snail or Slug subfamilies, and thus label it simply axolotl *snail*. Preparation of AP-2 riboprobe and in situ hybridization was as previously described (Epperlein et al., 2000). Axolotl Fgf8 cDNA was a gift from R. Christensen and R. Tassava (Christensen et al., 2001).

Image analysis

Whole-mount embryos were photographed under a stereomicroscope (Zeiss) with a Coolpix 950 camera. Sections were investigated under an epifluorescence microscope (Olympus BH 2). Separate brightfield and fluorescence images were captured with a SPOT RT

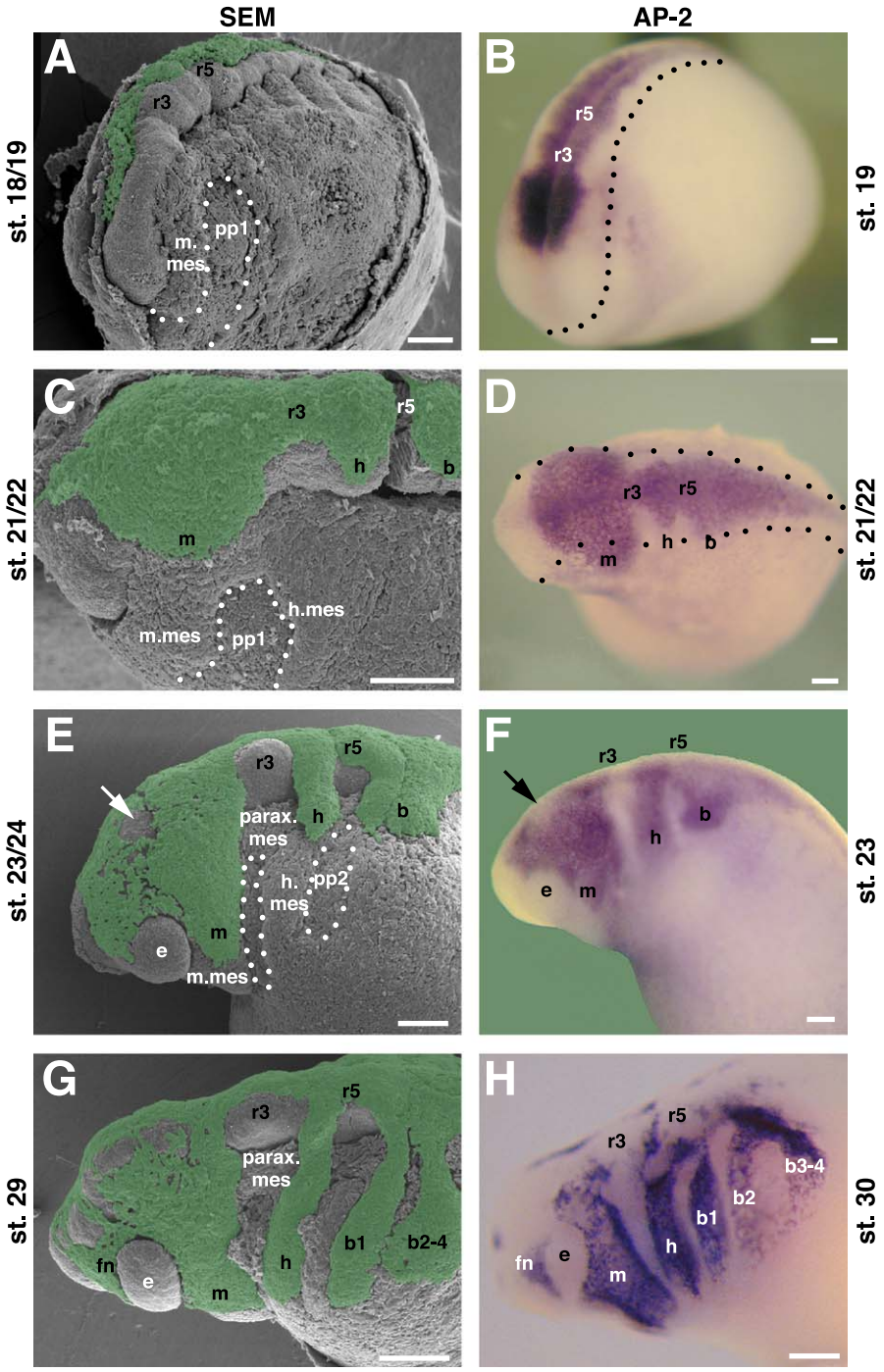

Fig. 1. Morphogenesis of cranial neural crest streams in the Mexican axolotl. (A, C, E, G) SEM micrographs of embryos after removal of the epidermis. The neural crest is colored green. (B, D, F, H) Embryos after hybridization with the AP-2 riboprobe. Head to the left in all cases. (A, B) Premigratory neural crest (stage 18/19). At prospective anterior brain levels, the neural crest is visible between the open neural folds; at the hindbrain, it forms the top of the fused folds. The dotted line in (A) outlines the first pharyngeal pouch (pp1) and in (B) the lateral border of the neural tube. Three heterogeneities are visible along the premigratory neural crest from which the future streams bulge out laterally. Fewer neural crest cells are found at rhombomere (r) r3 and r5. (C, D) Neural crest spreading (stage 21/22). The three initial neural crest bulges have spread laterally. Only the mandibular crest (m) has approached the mandibular mesoderm (m.mes). h, hyoid and b, common branchial neural crest stream, respectively. The dotted line in (C) delineates the dorsal part of the first pharyngeal pouch and in (D) the lateral border of the neural tube. (E, F) Formation of early neural crest streams (stage 23/24). The mandibular stream has migrated onto the mandibular mesoderm, the hyoid and common branchial stream over the paraxial mesoderm (parax.mes). Within the mesencephalon, another crest-free area is visible (arrows). In (E), the contours of the first two pharyngeal pouches are clearly visible (dotted lines). (G, H) Late neural crest migration (stage 29/30). The mandibular stream reaches its ventral-most position; the hyoid and branchial streams have reached a less ventral position. By comparing (G) with (E), the hyoid stream obviously follows the course of the hyoid mesoderm. The branchial stream shows subdivision. fn, frontonasal neural crest mass; b1, first branchial neural crest stream; b2–4, branchial neural crest streams 2–4; h.mes, hyoid arch mesoderm; pp2, pharyngeal pouch 2; e, eye. Scale bars, 200 μm.

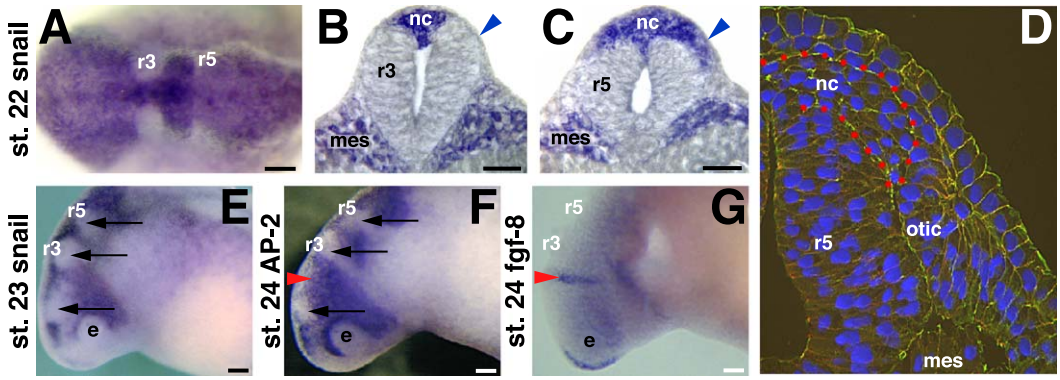

Fig. 2. Cranial crest-free spaces pattern neural crest streams. (A) Dorsal view of an embryo at stage 22 after hybridization with the Snail riboprobe showing early neural crest patterning. At r3, the neural crest string is very narrow; at r5, it is wider. (B, C) Transverse sections through the same embryo at r3 (B) and r5 (C). In contrast to r3, at r5 neural crest cells have migrated to a midventral position along the dorsoventral neural tube. The otic placode has not yet developed. Snail positive paraxial mesoderm (mes) is situated far away from early neural crest. (D) Soon after (at stage 24), the invaginated sensory layer of the otic placode (otic) inhibits neural crest migration from r5. Transverse section stained with anti-actin (red) and anti-β-catenin (green) antibodies (yellow in regions of overlay) to demonstrate tissue borders. DAPI (blue) visualizes cell nuclei. Red dots delineate neural crest. (E, F) From stage 23 onwards, another crest-free space arises rostral to r3 and r5 as observed with both neural crest markers (E, Snail; F, AP-2). Black arrows point to all three crest-free zones. (G) The position of the FGF-8 transcript (indicating the mid-hindbrain border) revealed that the new crest-free area is situated within the mesencephalon. The red arrowhead in (E and F) indicates the mid-hindbrain border. Scale bars, 100 μm.

camera, merged and optimized in Spot, MetaView and Adobe Photoshop software.

Results

Morphogenesis of cranial neural crest streams in the Mexican axolotl

We used morphological criteria in combination with molecular markers to determine neural crest migratory pathways (Fig. 1). By removing the epidermis, it is possible to identify neural crest cells by their morphology and arrangement under the scanning electron microscope (SEM). As molecular markers, we used AP-2 (Shen et al., 1997) and Snail (Essex et al., 1993), both of which exhibit a nearly identical expression in the axolotl neural crest. This represents the first molecular description of Snail expression in axolotl. In addition to the neural crest, Snail is expressed in the paraxial mesoderm (data not shown).

Premigratory neural crest

Around stage 18/19, the cranial neural crest first becomes morphologically recognizable (Figs. 1A,B) along the dorsal neural tube with the exception of the anteriormost portion, which remains neural crest-free throughout development. The width of the neural crest string varies at

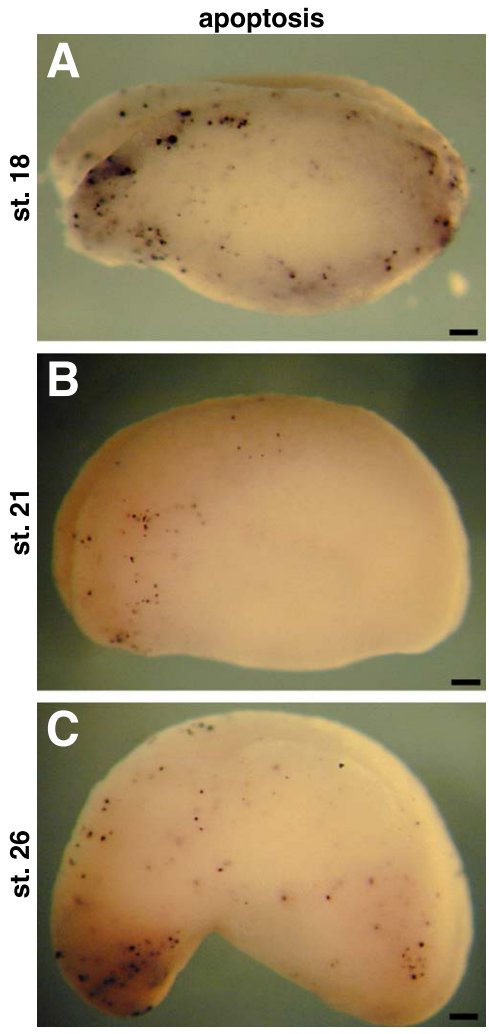

Fig. 3. Apoptosis has no influence on cranial neural crest patterning. TUNEL staining in axolotl embryos. Stages 18 (A), 21 (B) and 26 (C). Apoptotic cells are distributed randomly and do not display any relationship to rhombomeres or neural crest streams. Scale bars, 200 μm.

different axial levels. It is narrow at the future sites of rhombomeres (r) 3 and 5 but wider rostral to r3, within r4 and caudal to r5. The three wider areas develop into the mandibular, hyoid and common branchial neural crest streams.

Before the onset of neural crest migration, the cranial mesoderm spans from an area lateral to the neural tube ventrally to the prospective pharynx with the exception of the first endodermal pouch where endoderm contacts ectoderm. The first pouch divides the future pharyngeal part of the cranial mesoderm into an anterior and posterior area (Fig. 1A). The paraxial (dorsal) mesoderm is unsegmented anterior to r5, but develops into regular somites posterior to r5 (Fig. 1A).

Early stages of neural crest migration

The three presumptive neural crest streams spread laterally over the dorsolateral neural tube at stage 21/22 (Figs. 1C,D). The first bulge forms the future mandibular stream which moves over the paraxial mesoderm and approaches the arch mesoderm. The tongues of the hyoid and branchial neural crest streams have migrated only as far as to the lateral aspect of the neural tube and do not contact the paraxial mesoderm at this stage (Figs. 1C,D).

Around stage 23/24, early cranial neural crest streams have formed. The wide mandibular stream has migrated ventrally onto the arch mesoderm, whereas the hyoid stream is much shorter and narrower as it migrates over the paraxial mesoderm. It is similar in length but only one third the width of the common branchial stream (Fig. 1E).

By stage 23, the dorsolateral aspect of the neural tube becomes devoid of neural crest cells (Figs. 1E,F, arrow) anterior to the mid/hindbrain border (for details, see Fig. 2). Concomitantly, the second pharyngeal pouch evaginates (Fig. 1E) and contacts the ectoderm, whereby the hyoid arch mesoderm becomes separated from the posterior part of the branchial mesoderm.

Late neural crest migration

At stage 29–30, the wide mandibular stream has reached its ventral-most extent, whereas the narrow hyoid and individual branchial neural crest streams are still progressing ventrally (Figs. 1G,H). The anterior part of the mandibular stream migrates into the frontonasal process, whereas the posterior, postoptic neural crest contributes to the first pharyngeal arch. The common branchial stream and branchial mesoderm gradually become subdivided (Figs. 1G,H) by local outgrowth of the endoderm and ingrowth of the epidermis. At stage 29/30, AP-2 (Figs. 1H) and Snail (not shown) appear to be decreased in the dorsal portions of the neural crest streams but stain strongly in the ventral portions. This may be due to down-regulation of neural crest markers (Epperlein et al., 2000) and/or a depletion of cranial neural crest cells which aggregate into the primordia of sensory ganglia (Northcutt and Brändle, 1995).

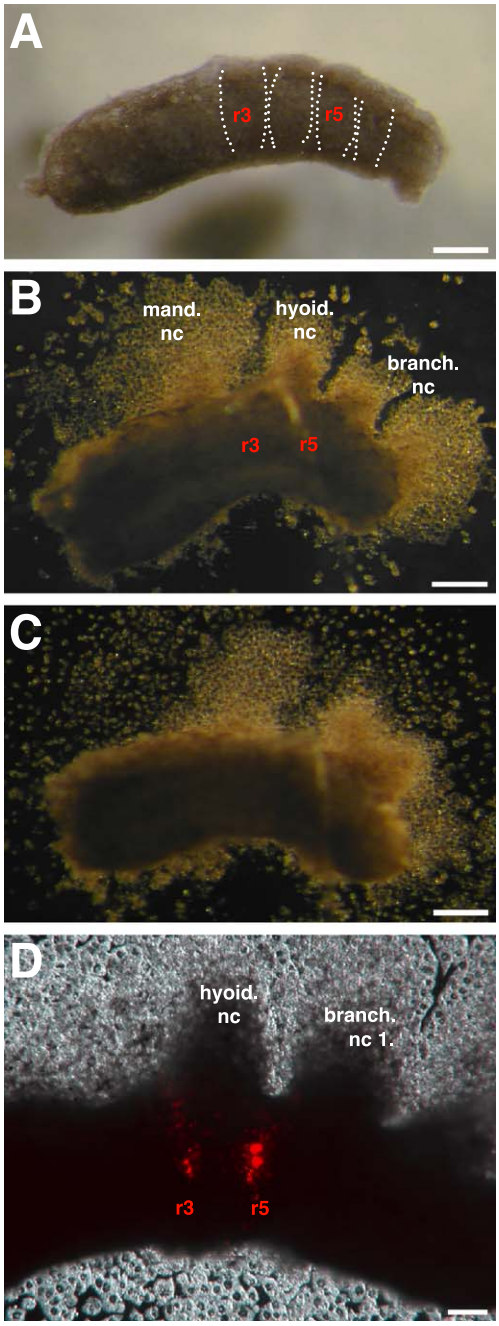

Fig. 4. Cranial neural tube explants can produce distinct neural crest streams. (A) Excised cranial neural tube, anterior to the left, stage 21. White dots outline the borders of rhombomeres. (B) The same tube 20 h later on a fibronectin-coated substrate. Neural crest cells migrate out laterally in well-defined streams without being influenced by other tissues. (C) The same specimen about 35 h later. Streams are now fused. (D) Enlarged view of a different culture 15 h after the rhombencephalon was labeled with DiI at the position of r3 and r5. Some neural crest cells migrate from r3 and r5 but join streams from all even numbered rhombomeres. mand.nc; hyoid.nc; branch.nc; branch.nc.1., mandibular, hyoid, branchial and the first branchial neural crest stream, respectively. Scale bars: 200 μm in (A–C), 100 μm in (D).

Neural crest-free regions along the head neural tube pattern early neural crest streams

There are two principal neural crest-free areas adjacent to r3 and r5 that pattern early neural crest streams (Fig. 2A). At r3, neural crest cells form only the middle part of the neural tube roof and do not migrate laterally (Fig. 2B). In contrast, they cover the entire roof at r5 and have migrated half way down the neural tube (Fig. 2C). Subsequently, the sensory layer of the otic placode starts to invaginate at r5 and limits neural crest migration (Fig. 2D). Detailed cellular analysis of sectioned embryos hybridized with AP-2 and Snail (not shown) as well as of embryos stained for actin and β-catenin (Fig. 2D) reveal that no neural crest cells migrate between the otic placode and r5.

Using SEM (Fig. 1E; $n = 4$) as well as Snail (Fig. 2E; $n = 5$) and AP-2 in situ hybridization (Fig. 2F; $n = 11$), we noted another neural crest-free space in the dorsal cranial neural crest from stage 23 onwards. To accurately determine the rostrocaudal level of this space, we compared embryos stained for AP-2 and FGF-8 transcripts to indicate the position of the mid-hindbrain border (Figs. 2F,G; Han et al., 2001; Riou et al., 1998). It is likely that this neural crest-free space is situated within the mesencephalon, anterior to the mid-hindbrain border and may contribute to patterning of the mandibular neural crest.

Apoptosis and local cell proliferation have no apparent influence on early cranial neural crest patterning

In avian embryos, it has been proposed that localized cell death eliminates cranial neural crest precursors at r3 and r5 and thus patterns neural crest cells into streams

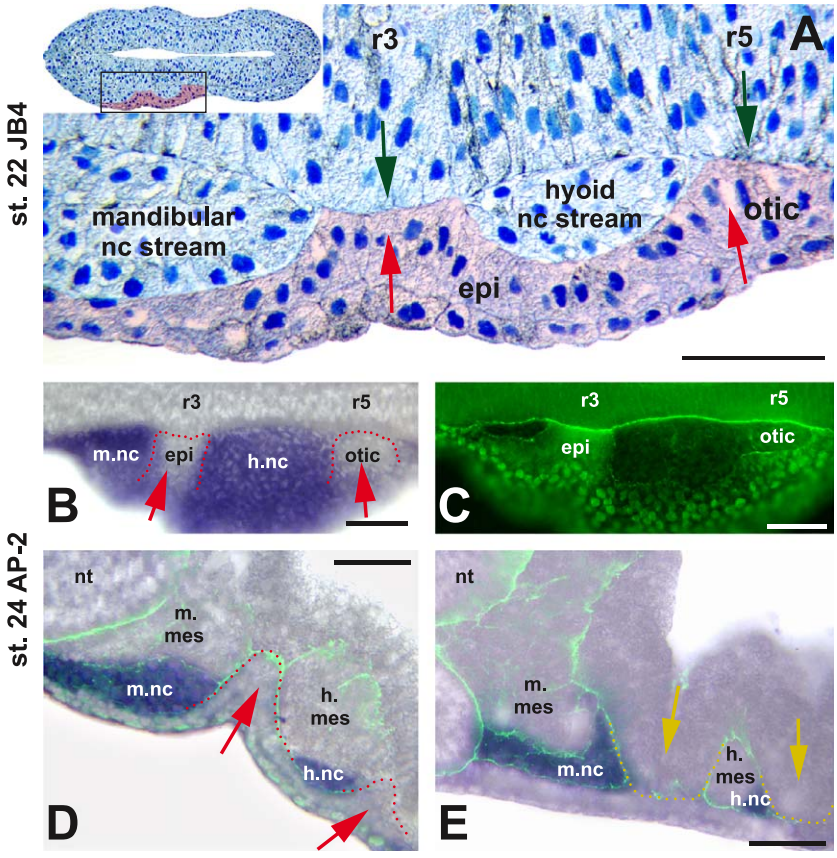

Fig. 5. Neural crest streams are constrained in tissue channels (anterior to the left, only left side shown in all cases). (A) Horizontal plastic section through the neural tube of an embryo at stage 22. The frame within the small inset indicates the position of the enlarged image. The epidermis (epi, colored red) invaginates and contacts the neural tube epithelium intimately at r3 and r5. Thus, channels are formed through which neural crest streams are directed. Red arrows show epidermal invaginations; green arrows show the bulging neural tube at r3 and r5. (B, C) Horizontal vibratome section through the neural tube at stage 24 after in situ hybridization with the AP-2 riboprobe. The mandibular neural crest (m.nc) and hyoid neural crest (h.nc) streams are stained. (C) shows the same section after counterstaining with anti-fibronectin to reveal tissue borders. Images in (A–C) demonstrate identical epidermal invaginations (red arrows and dotted lines in B) in two different embryos constraining neural crest migration. (D, E) Horizontal sections through the dorsal (D) and ventral (E) pharynx (the same embryo as B and C). The sections with the AP-2 riboprobe were counterstained with anti-fibronectin (green) to reveal tissue borders. Dorsally, at a paraxial level (D), the epidermis invaginates in register with r3 and r5 (red arrows and dotted lines) and divides mandibular from hyoid crest. Ventrally (E), the first and the second endodermal pouches (yellow arrows and dotted lines) evaginate in register with r3 and r5 and keep neural crest streams separate. otic, otic placode; nt, neural tube; m.nc, mandibular neural crest; h.nc, hyoid neural crest; m.mes, mandibular arch mesoderm; h.mes, hyoid arch mesoderm. Scale bars, 5 μm in (B and C), rest 100 μm.

(Graham et al., 1993). To investigate whether programmed cell death contributes to neural crest patterning in the axolotl, we used TUNEL to determine the distribution of apoptotic cells in albino embryos. Randomly distributed dying cells were observed through development (Fig. 3), with no obvious increase of apoptosis adjacent to r3 or r5. The same was observed on sections (not shown). As positive controls (not shown), similar staining in chick limb buds revealed cell death as expected in the interdigital zone (Zou and Niswander, 1996) and in *Xenopus* embryos comparable to that described in previous publications (Hensey and Gautier, 1998).

To examine whether regionally different rates of neural crest proliferation are involved in the control of cranial neural crest migration, proliferating cells were identified using an anti-Phosphohistone-3 antibody (data not shown). Many positive epidermal cells were observed, with no obvious regional differences. After removal of the head epidermis, positive cells (very likely neural crest) were found randomly scattered along the dorsal neural tube. Within the pharyngeal neural crest streams, the density of mitotic cells was higher than in adjacent mesodermal tissue. Therefore, there is extensive proliferation in the neural crest population but no obvious regional specificity to the proliferation.

Cranial neural tube explants produce distinct neural crest streams in vitro

Cranial neural crest cells move in a segmental fashion through adjacent tissues. This segmentation may be inherent to the migrating cells themselves and/or imposed by neighboring tissues. To investigate neural crest migratory patterns in the absence of other tissues, cranial neural

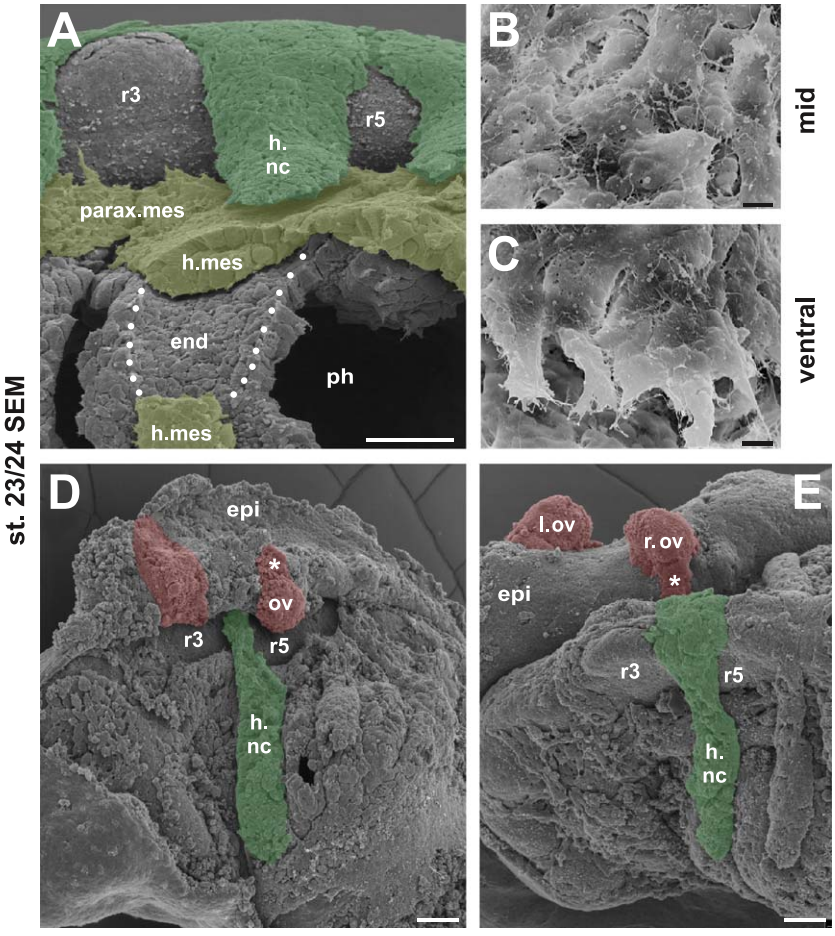

Fig. 6. Shape and constraints of cranial neural crest streams. (A) Pseudo-colored SEM micrograph of an epidermis-ablated embryo at stage 23/24 (head to the left outside); neural crest cells are colored green and mesoderm yellow. Notice the compactness of the hyoid stream (h.nc). The dotted lines delineate part of the hyoid arch mesoderm (h.mes) which was removed to expose the endoderm (end). (B, C) Details of neural crest cell shape in the middle (B) and at the leading edge (C) of the migrating hyoid stream. Only those cells at the leading edge show an obvious dorsoventral orientation that suggests an active ventral cell movement. (D, E) SEM micrographs of embryos in which the epidermis (epi) was unfolded to show the strong ectodermal invagination of the otic vesicle (ov) with its ventral extension (asterisk) at r5 (colored red) and of another dorsoventral invagination of the epidermis at r3 (colored red). These epidermal barriers keep neural crest streams apart. For clarity, the hyoid neural crest stream is colored green. l.ov, left otic vesicle; r.ov, right otic vesicle; parax.mes, paraxial mesoderm. Scale bars, 5 μm in B and C, rest 100 μm.

tube explants were grown in tissue culture on a permissive substrate. The cranial ectoderm was removed from embryos at the earliest stages of neural crest migration (stages 20–22) and the cranial neural tube was carefully excised and placed on a fibronectin-coated substrate (Fig. 4A). Surprisingly, even in isolation, neural crest cells migrated in distinct streams (Fig. 4B) and maintained this separation for at least 30 h. However, neural crest cells became nearly confluent with little or no obvious separation at later times (Fig. 4C). DiI labeling of r3 and r5 reveal that the gaps in migration are across from the odd numbered rhombomeres (Fig. 4D). Some labeled neural crest cells emerged from r3 and r5 and joined migratory streams from even numbered rhombomeres (Fig. 4D), as

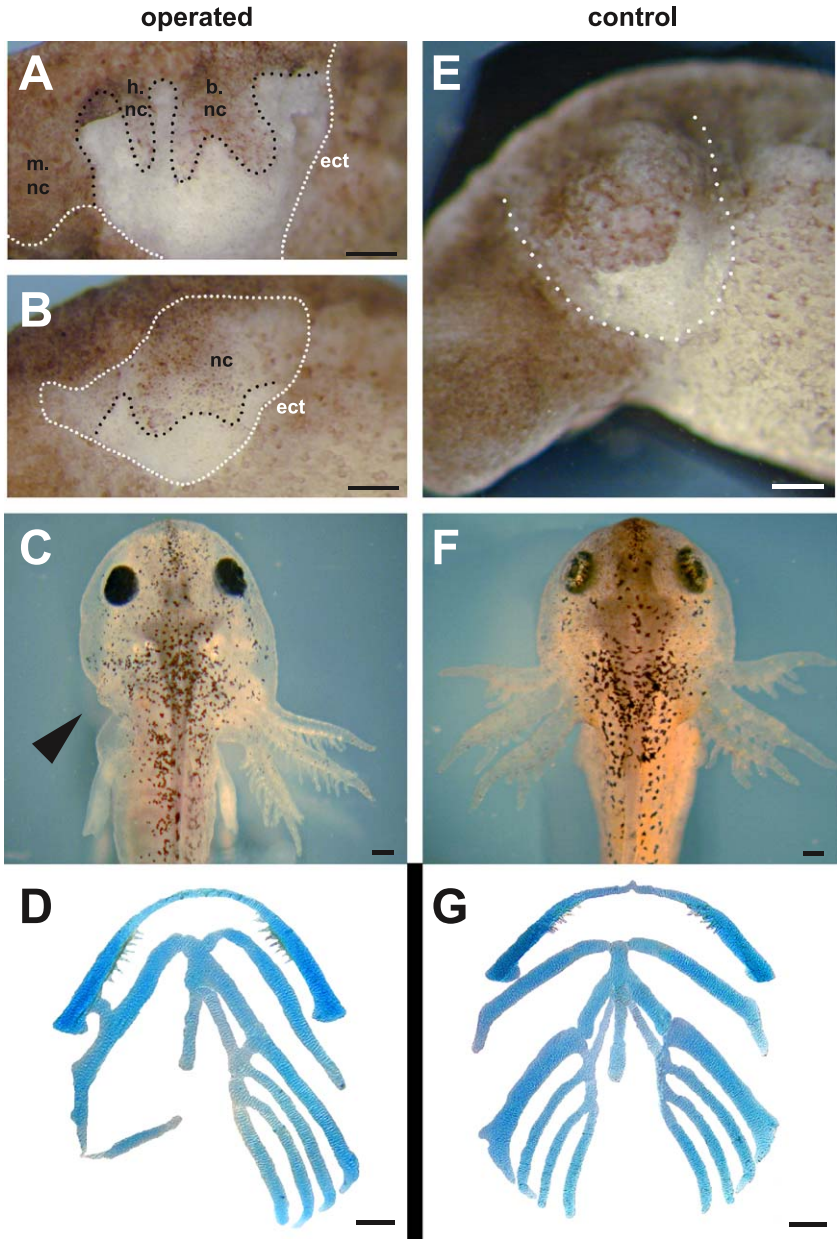

Fig. 7. Removal of the head epidermis stops neural crest migration and perturbs normal patterning of the visceral skeleton. (A, B) Lateral views of an embryo in which the dorsolateral part of the head epidermis was removed at stage 24 (A). Black dotted line delineates neural crest, which contrasts against the white mesoderm because of pigment granules. The white dotted line delineates part of the ectodermal area (ect) removed. (B) Seven hours later, the white dotted line delineates ectoderm-free area. Without the epidermal covering, neural crest streams fuse. (C) Four days later, the epidermis regenerated and covered the wound but did not develop into outer gills (arrowhead). (D) Alcian blue staining of the specimen's visceroskeleton 10 days later; lack of cartilages on the operated side. (E) Control embryo at stage 26, lateral view. The epidermis was lifted but replaced immediately. White dots delineate the operated area. (F) Four days later, the outer gills of the larva are developed in the same way on the operated side as on the control side. (G) Alcian blue staining of the control specimen, 10 days later showing normal development of viscerocranial skeleton on both sides. m.nc, mandibular; h.nc, hyoid; b.nc, branchial neural crest streams. Scale bars, 200 μm.

has been previously reported in vivo (Sechrist et al., 1993).

Tissue channels reinforce distinct cranial neural crest streams

The fact that cranial neural crest cells have an inherently segmental migratory pattern raises the interesting question of whether or not the tissue environment also influences migration. To examine this question, we carefully analyzed the relationship between neural crest cells and surrounding tissue using a combination of high-resolution light microscopy and SEM. As soon as neural crest cells initiate their migration from the dorsal neural tube, they appear in condensed streams (Figs. 1C,D) interposed between regions where the neural tube is tightly apposed to the ectoderm at the levels of r3 and r5 (Fig. 5A). This continues along the dorsoventral axis such that the outer epidermis and internal tissues (neural tube, mesoderm and endoderm) are locally closely apposed. This produces several dorsoventrally oriented apposition zones that create adjacent channel-like spaces through which neural crest streams migrate. These tissue barriers are visible from the beginning of neural crest cell migration (stage 22, Fig. 5A), becoming progressively more evident at later stages (stage 24, Figs. 5B–E). For example, at a dorsal level, the epidermis and the dorsolateral neural tube are closely apposed at the neural crest-free regions of r3 and r5 (Figs. 5B,C). Further, ventral to these spaces, intimate contact exists between the thickened and invaginated epidermis and the paraxial mesoderm (Fig. 5D). Still more ventrally, the first and second endodermal pouches appose the epidermis (Fig. 5E). The first pouch forms in register with the neural crest-free space at r3, the second pouch in register with r5.

Scanning electron microscopy was used to visualize the tissue appositions and channels in a three-dimensional manner (Figs. 6A,D,E). These images reveal the presence of continuous dorsoventral apposition zones first between ectoderm and neural tube and then between ectoderm, mesoderm and endoderm as they progress ventrally. Neural crest streams are present extending from dorsal to ventral between these apposition zones. Within the streams, individual migrating neural crest cells appear polygonal in shape (Fig. 6B), with no obvious orientation. In contrast, neural crest cells at the leading edge of the streams appear oriented dorsoventrally and have numerous filopodia (Fig. 6C).

Following removal of the epidermis, cranial neural crest streams fuse, and the pattern of the visceral skeleton is perturbed

The above results suggest that formation and maintenance of neural crest streams involve intrinsic patterning information together with a structural importance for neighboring tissues. To test a possible role for the epidermis in formation or maintenance of neural crest streams, we removed the dorsolateral region of the head epidermis at stages 23–26 (Fig. 7A; n = 15). Following such an operation, neural crest streams stop their lateral movement, lose their compact configuration, and become confluent after 3–8 h (Fig. 7B). About 4 days later, regenerated epidermis has grown over the ablated area but fails to support the formation of outer gills (Fig. 7C) and proper viscerocranial cartilage (Fig. 7D). To assure that the development of these structures did not fail because of a lack of neural crest cells that were detached during epidermis removal, the epidermis was detached and then repositioned after a brief lifting (Fig. 7E). In these control embryos (n = 7), outer gills (7/7) and visceral cartilage (5/7) developed normally (Figs. 7F,G). These results suggest that neural crest–epidermal interactions are necessary for maintenance of cranial neural crest cell migration in streams and for their continuous migration.

Cranial neural crest cells only migrate laterally and do not mix with mesoderm

SEM analysis suggests that neural crest streams leaving the neural tube continue to spread on the outside of the paraxial and arch mesoderm (Fig. 6A). However, the precise relationship between migratory neural crest and mesoderm cannot be determined by SEM. Therefore, we analyzed sections of embryos hybridized with neural crest markers AP-2 or Snail. The latter also stains paraxial, but not branchial arch, mesoderm. The axolotl Snail expression pattern is highly reminiscent of Snail and Slug in *Xenopus* (Mayor et al., 1995).

We focused on neural crest migration at the hyoid (r4) level because of its optimal visibility. At stage 22, (Figs. 8A,B), neural crest cells cover the dorsolateral surface of the neural tube. By stage 23 (Figs. 8C,D), the hyoid stream reaches the paraxial mesoderm where it turns laterally but not medially (between the mesoderm and neural tube). Later, at the pharyngeal level, the hyoid stream migrates on the outside of the arch mesoderm (stage 26, Figs. 8E,F). No mixing of neural crest cells with mesoderm was observed at either paraxial or pharyngeal levels.

Because molecular markers are not definitive lineage markers, we directly labeled cranial neural crest cells with lineage tracers to visualize their relationship with surrounding tissue. First, focal injections of DiI were performed into the cranial neural folds. Second, two- to four-cell stage embryos were injected with GFP mRNA, grown to the neurula stage and then GFP-labeled head neural folds were transplanted to unlabeled host embryos. Both these techniques

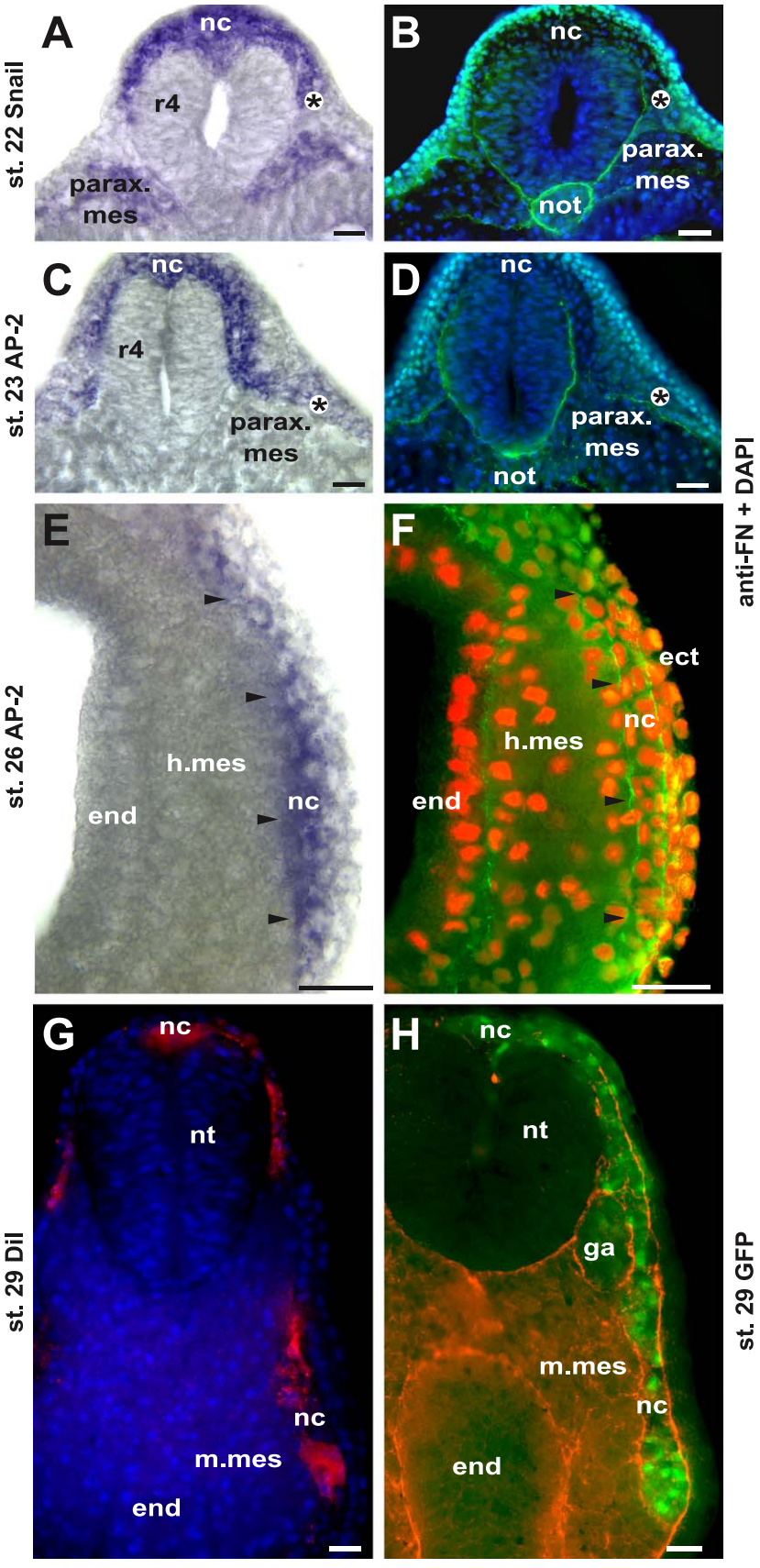
A
nc
r4
parax.
mes
B
nc
parax.
mes
not
st. 22 Snail
C
nc
r4
parax.
mes
D
nc
parax.
mes
not
st. 23 AP-2
E
h.mes
nc
end
F
ect
nc
h.mes
end
anti-FN + DAPI
st. 26 AP-2
G
nc
nt
nc
m.mes
end
H
nc
nt
ga
m.mes
nc
end
st. 29 DiI
st. 29 GFP

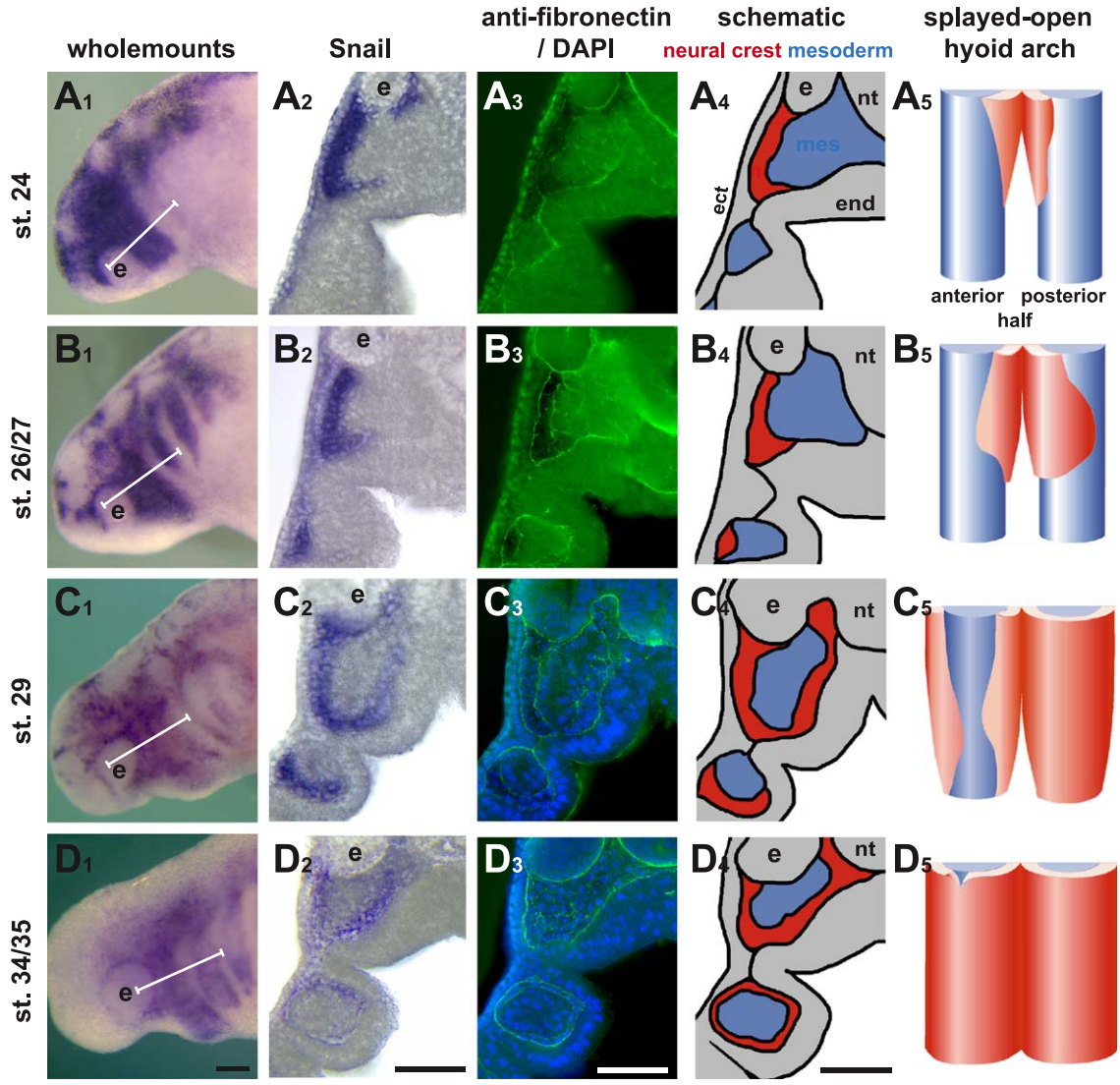

Fig. 9. Outside-in movement of neural crest cells during pharyngeal arch morphogenesis. First column shows embryos after hybridizing with the Snail riboprobe at stages 24 (A), 26/27 (B), 29 (C) and 34/35 (D). White lines indicate the position of horizontal sections shown in column 2 (left half and mandibular and hyoid areas shown only). Sections were made at six to eight different horizontal planes along the dorsoventral axis; of these always a middle one is shown at the level of the eye vesicle (e). Column 3 shows the same sections after counterstaining with anti-fibronectin (anti-FN) and DAPI; column 4 summarizes the previous information and column 5 offers a 3D view of the ensheathment of left hyoid mesoderm (blue) with neural crest (red). In column 5, the anterior part of the arch was unfolded and turned to the left; the posterior part stayed in place. From their subepidermal position, neural crest cells migrate deep into the arches around the mesodermal core but do not mix with it. Neural crest cells start to migrate from a posterolateral position around the arch mesoderm both anteriorly (shown on the left half of the arch) and posteriorly (right half). The anterior encirclement is delayed. ect, ectoderm; end, endoderm; nt, neural tube; e, eye. Scale bars, 200 μm.

demonstrated a definite segregation between labeled neural crest cells and adjacent mesoderm (Figs. 8G,H). Thus, molecular markers as well as direct cell marking demonstrate that axolotl neural crest cells migrate over but do not intermix with mesodermal tissues.

Fig. 8. Neural crest cells migrate only laterally and do not mix with mesoderm. (A–D) Transverse sections through r4 showing early migration of the hyoid neural crest stream at stages 22 (A, B) and 23 (C, D). In (A), both neural crest and paraxial mesoderm (parax.mes) are Snail positive. The lateral front of neural crest cells (asterisk) has not yet reached the paraxial mesoderm. (B) Counterstaining of the same section with anti-fibronectin (green) and DAPI (blue). At stage 23 (C), AP-2 positive neural crest cells (asterisk) have moved laterally but not medially toward the notochord (not). (D) Counterstaining of the same section as in C. (E, F) Transverse section (detail) through a hyoid arch at stage 26. (E) Neural crest cells are hybridized with the AP-2 riboprobe. (F) Counterstaining of the same section as in (E), but DAPI was converted into red. Neural crest cells migrate only on the outside of the hyoid arch mesoderm (h.mes) and do not invade it (black arrowheads demarcate the border between neural crest and mesoderm). (G) Transverse section through a DiI-injected embryo (stage 29) through the mandibular arch. Neural crest cells (red) migrate only along the lateral pathway. Counterstained with DAPI (blue). (H) Same situation as in (G), all neural crest is stained by GFP (green). Counterstained with anti-fibronectin (red). m.mes, mandibular mesoderm; end, endoderm; ect, ectoderm; nt, neural tube; ga, ganglion. Scale bars: 100 μm.

Cranial neural crest streams conduct an outside-in movement during pharyngeal arch morphogenesis

We have shown that initially, cranial neural crest cells migrate subepidermally, neither mixing with mesoderm nor migrating along a medial pathway (Fig. 8). Later, neural crest cells are found deep within the pharyngeal arches. Our analysis at the level of the mandibular and hyoid arch shows that they reach this location by migrating inward around the mesodermal arch cores in an ''outside-in'' movement (Fig. 9) during which no mixing occurs between neural crest cells and mesoderm. More posterior arches develop in essentially the same manner, though the number of cells in individual arches is lower and therefore this process is not as clearly visible.

Initially, neural crest cells occupy a lateral position on the outer mesodermal surface (Fig. 9A, stage 24) as can be envisioned by the Snail signal (Fig. 9A1,2). After reaching their ventral-most position within the arch, the neural crest cells turn medially and gradually ensheath the arch mesoderm (Figs. 9B–D). The inward movement of neural crest cells starts from a posterolateral level (Figs. 9B,C) before lateral migration is completed. Finally (Fig. 9D, stage 34/35), the entire central mesoderm is homogeneously enveloped by neural crest cells. As they migrate, they increase their contact area with pharyngeal endoderm. The ensheathment process of a single hyoid arch is illustrated in a 3D reconstruction (Fig. 9). A splayed-open view of the ventral portion of the hyoid arch illustrates how neural crest cells (red) migrate around but do not mix with the mesodermal arch core (blue).

Because molecular markers are not true lineage markers, we next confirmed the outside-in movement of neural crest cells using cell marking techniques. Embryos were labeled either with rhodamine dextran or GFP mRNA at the two-cell stage. Embryos were allowed to develop until the neurula stage at which time one of the neural folds was grafted isotopically into an unlabeled host. For both types of lineage label, similar results were observed (data not shown). Labeled neural crest cells were initially seen along the lateral pathway. At subsequent times, they appeared to ensheath the mesoderm in an outside-in manner identical to that observed with molecular markers for neural crest, AP-2 and Snail.

Discussion

The global pattern of cranial neural crest migration in axolotl closely resembles that of other vertebrates (Lumsden et al., 1991; Meulemans and Bronner-Fraser, 2002; Olsson et al., 2002; Sadaghiani and Thiébaud, 1987; Trainor et al., 2002) and might suggest a broad conservation of basic patterning mechanisms. However, numerous specific properties of cranial neural crest cell migration are distinctly different among vertebrates (e.g., Serbedzija et al., 1992; Trainor et al., 2002). Therefore, it is essential to perform analyses across divergent species to uncover the fine regulation of patterning, and to determine which mechanisms are controlled intrinsically versus extrinsically by the environment.

Patterns of premigratory and early migrating cranial neural crest

In axolotl, the premigratory cranial neural crest appears as a ''string'' of variable thickness on the dorsal side of the neural tube in the late neurula (Figs. 1A,B). The wider portions of the string give rise to the three principal neural crest streams: the mandibular, hyoid and common branchial stream (Falck et al., 2002).

Once cells initiate migration, there are several regions from which migrating neural crest cells are conspicuously absent: one in the mesencephalon and two in the rhombencephalon adjacent to r3 and r5 (Fig. 2). Rhombomere 3 separates the mandibular from the hyoid and r5 the hyoid from the common branchial neural crest stream. The mesencephalic neural crest-free space is likely to separate the maxillo-mandibular arch neural crest from the more anterior, frontonasal neural crest (Figs. 1G,H). Despite its presence in illustrations of whole mounts of frog, chick and mouse (Alfandari et al., 2001; Chai et al., 2000; Kuratani and Eichele, 1993; Linker et al., 2000; Mayor et al., 1995; Osumi-Yamashita et al., 1994; Robinson et al., 1997; Sadaghiani and Thiébaud, 1987; Serbedzija et al., 1992), the mesencephalic neural crest-free space has not been described previously. Several mechanisms may account for the formation of neural crest-free spaces and subsequent patterning of streams. These include apoptotic elimination (Graham et al., 1993), selective proliferation, tissue interactions such as paraxial exclusion zones (Farlie et al., 1999) and/or specific signaling molecules such as Eph/ephrin interactions (Holder and Klein, 1999; Robinson et al., 1997; Smith et al., 1997), FGF2 (Kubota and Ito, 2000) or *collapsin 1* (Eickholt et al., 1999).

In axolotl, the random distribution of apoptotic cells (Fig. 3) is inconsistent with a role for cell death in shaping neural crest streams. In the chick, neural crest cells at r3 and r5 have been proposed to undergo cell death (Hirata and Hall, 2000; Lumsden et al., 1991) mediated by *BMP-4* and *Msx-2* (Graham et al., 1993; Smith and Graham, 2001). However, the influence of apoptosis on early neural crest patterning is controversial, not only in chick (Farlie et al., 1999) but also in zebrafish (Cole and Ross, 2001; Ellies et al., 1997), *Xenopus* (Hensey and Gautier, 1998) and mice (Trainor et al., 2002).

A regionally different rate of neural crest proliferation is another possible cell-intrinsic mechanism that might pattern neural crest streams. However, we found no differences in the rate of proliferation between even and odd rhombomeres using an anti-Phosphohistone-3 antibody (Hendzel et al., 1997; Saka and Smith, 2001). In frog, chick and mouse

embryos, there is some evidence that r5 generates more neural crest cells than r3 (Anderson and Meier, 1981; Robinson et al., 1997; Sechrist et al., 1993; Trainor et al., 2002). However, this is unlikely to influence the patterning of neural crest cell migration.

Intrinsic properties contribute to segmental migration of cranial neural crest

We explored the possibility that cranial neural crest cells themselves may contribute to the observed segmental migration in the hindbrain by examining their behavior in isolation. To this end, cranial neural crest cells from stage 20–22 embryos were grown on fibronectin-coated substrates in vitro. Surprisingly, we found that streams of neural crest cells from r2, r4 and r6 were clearly visible even in the absence of neighboring tissue. The streams remained separate for at least 30 h, becoming fused thereafter (Fig. 4). Thus, early steps of cranial neural crest cell migration and subsequent patterning into separated streams appear to be autonomous. These data suggest that there are indeed intrinsic differences between adjacent neural crest populations that may lead to sorting behavior and thus contribute to the genesis of neural crest streams.

When r3 and r5 cells were labeled focally with DiI, it was clear that the gaps in migration corresponded to the odd numbered rhombomeres. However, DiI-labeled neural crest cells emerged from these rhombomeres, but joined the streams of neural crest cells from even numbered rhombomeres (Fig. 4D). This is consistent with in vivo labeling experiments in chick and mouse, suggesting that r3 and r5 generate neural crest cells that are redirected anteriorly or posteriorly joining the lateral streams from r2, r4 and r6 (Birgbauer et al., 1995; Kulesa and Fraser, 2000; Trainor et al., 2002).

What molecular properties might account for the separation of adjacent neural crest populations even in the absence of other tissue types? In *Xenopus*, the complementary expression of Eph receptors and ligands in adjacent populations of migrating neural crest cells appears to segregate streams and ensure neural crest migration into the correct arch (Holder and Klein, 1999; Smith et al., 1997). At later stages, other molecules may contribute to neural crest migration; for example, FGF8 is known to affect the morphogenetic movements of the pharynx and subsequent segregation of neural crest streams (Trumpp et al., 1999).

Tissue interactions help maintain segmental migration of cranial neural crest

We explored the possibility that interactions between neural crest and adjacent tissues might influence neural crest migration and patterning. In other systems, paraxial mesoderm is favored for influencing neural crest migration (Farlie et al., 1999; Noden et al., 1999; Trainor and Krumlauf, 2000a; Trainor et al., 2002). However, in axolotl, cranial neural crest cells migrate and form streams well before they reach the paraxial mesoderm (Figs. 1C,D, 2 and 5A–C). This makes it clear that the mesoderm has no influence on initial steps of neural crest cell migration. Its migration, however, might have been influenced by interactions between the neural tube surface and epidermis and/or may be an autonomous process as suggested from observations in culture (Fig. 4).

Interestingly, we observed apposed thickenings of the neural tube and epidermis adjacent and ventral to r3 and at r5 that form well-defined exclusion zones for migrating neural crest cells (Figs. 5 and 6). Careful analyses revealed tight appositions between zones of adjacent tissues in register with r3 and r5 (Fig. 5). This results in the formation of a "channel" adjacent to r4 through which hyoid neural crest cells migrate ventrally. Similar channels form at the mandibular and branchial levels as well. Such exclusion zones have been previously proposed though not understood mechanistically (e.g., Farlie et al., 1999). A similar barrier mechanism had been documented for the otic placode at r5 before in fish (Sadaghiani and Vielkind, 1989), newt (Jacobson and Meier, 1984), turtle (Meier and Packard, 1984), chick (Sechrist et al., 1993) and mouse (Trainor et al., 2002). Our data suggest that such zones exist for r3 as well as r5 in axolotl. In both odd numbered rhombomere regions, migrating neural crest cells are mechanically constrained. In species in which the otic placode initially develops closer to r4, a conspicuous neural crest stream migrates from r5 (Bradley et al., 1992; Del Pino and Medina, 1998; Horigome et al., 1999; Sadaghiani and Thiébaud, 1987). This supports the idea that extrinsic mechanisms are important for regulating neural crest migration. Moreover, grafting r5 to other locations results in lateral migration of r5-derived neural crest cells (Saldivar et al., 1996; Trainor et al., 2002) and extirpation of epidermis at r3 leads to the lateral migration of neural crest cells from r3 (Golding et al., 2002). When small grafts from the paraxial area consisting of cranial mesoderm or surface ectoderm were transplanted next to r4, they were unable to inhibit neural crest cell migration (Trainor et al., 2002). Therefore, these tissues do not appear to secrete inhibitory signals. We conclude that at the beginning of cranial neural crest migration, mechanical interactions between the neuroepithelial and the epidermal layer create well-defined neural crest-free zones that maintain streams of neural crest cells in channels between neighboring tissues.

Our results show that there are regions through which the cranial neural crest cells can migrate with facility, that arise between regions of close apposition that appear to block neural crest migration. These channels are likely to result partially from mechanical influences of the environment but may also be created by the migrating neural crest cells themselves burrowing their way through permissive tissue.

Tissue channels help to guide neural crest cells to the pharynx

Our results demonstrate that cranial neural crest cells migrate laterally in compact streams in which they are funnelled through adjacent tissues en route to the pharynx (Fig. 5). As nicely illustrated in the chick (Veitch et al., 1999), pharyngeal arch patterning is not coupled to neural crest migration and cranial tissue is regionalized even in the absence of the neural crest. Similarly in zebrafish, the endoderm has been suggested to form segment boundaries between arches to constrain neural crest migration (Schilling and Kimmel, 1994). Moreover, in the zebrafish *vgo* mutant, pharyngeal endoderm does not form pouches and consequently neural crest streams fuse at a ventral (pharyngeal) but not dorsal level where neural crest cells migrate in normal streams (Piotrowski and Nüsslein-Volhard, 2000).

We find that ablating the cranial epidermis in axolotl causes fusion of neural crest streams and finally cessation of neural crest migration (Fig. 7). These results suggest that interactions between both ectoderm and endoderm may be critical for neural crest migration in streams. Without directed navigation of neural crest streams through the ecto-/endodermal interface, cranial neural crest cells cannot reach their final destinations and ectomesenchymal derivatives fail to develop properly (Fig. 7D). We assume that this mechanical interaction is a main part of common evolutionary conserved mechanisms which keep cranial neural crest streams separate and guide neural crest cells along correct pathways during craniofacial development of vertebrates.

Outside-in movement

The embryonic pharyngeal arch of vertebrates consists of a central mesodermal core ensheathed by neural crest (e.g., Hacker and Guthrie, 1998; Meulemans and Bronner-Fraser, 2002; Noden et al., 1999; Trainor and Tam, 1995). However, the precise spatiotemporal order in which both tissues interact during arch morphogenesis is not known.

We have shown that cranial neural crest streams in axolotl migrate exclusively along the lateral (subepidermal) pathway and neither mix with mesoderm nor use a medial route (Fig. 8). This seems to be a unique feature of axolotl embryos, since in other vertebrates in addition to the predominant lateral route, neural crest cells invade the cranial mesoderm (e.g., Noden, 1988; Noden et al., 1999; Sadaghiani and Thiébaud, 1987; Serbedzija et al., 1992; Tan and Morris-Kay, 1986; Trainor and Tam, 1995). However, the exact way that the mesoderm becomes eventually ensheathed by neural crest cells is not known. Kimmel et al. (2001) have put forth an elegant model in zebrafish suggesting that neural crest cells migrate laterally along the arch mesoderm and encircle it by moving from "outside-in".

Here, we document for the first time in gnathostomes the dynamic development of an arch ensheathment via an outside-in movement of neural crest cells (Fig. 9) that supports the model proposed by Kimmel et al. (2001). In the axolotl, neural crest streams initially move subepidermally. At a pharyngeal level, however, neural crest streams turn medially circumnavigating the mesodermal core of each arch and progress toward the pharyngeal endoderm, first from a posterior, then from an anterior location, and in a slight ventral to dorsal fashion. In this manner, the entire arch mesoderm becomes encircled by neural crest cells. The two cell types do not intermix nor do neural crest cells use a medial pathway as in the trunk. The ventral to dorsal fashion in which axolotl cranial neural crest cells envelop the arch mesoderm reminiscent of the manner in which cranial and trunk neural crest cells colonize their derivatives in chick and mouse (Lumsden et al., 1991; Serbedzija et al., 1989, 1992). Early migrating neural crest cells first populate the ventral branchial arches, later ones the mid-pharynx, whereas the latest contribute to sensory ganglia situated dorsally.

In contrast to previous views (e.g., Kimmel et al., 2001), cranial neural crest cells were observed to completely surround the mesodermal core of branchial arches in lamprey, a basal agnathan vertebrate (McCauley and Bronner-Fraser, 2003; Meulemans and Bronner-Fraser, 2002). Thus, this resolves the long-standing controversy of whether neural crest cells are being distributed around the mesoderm. However, many differences between gnathostomes and agnathans are still apparent: lamprey neural crest cells fail to fill their derivatives in a ventral to dorsal order and a medial migratory route of cranial neural crest cells is clearly observed (McCauley and Bronner-Fraser, 2003). Thus, the neural crest sheaths around the arches appear to be an ancient and conserved vertebrate trait, whereas the ventral-to-dorsal filling of derivatives appears to have arisen after the agnathan/gnathostome transition. Still more precise neural crest cell tracing experiments are needed in both vertebrate groups to understand how developmental pathways were changed during the agnathan/gnathostome transition. One might speculate that the failure of cranial neural crest cells to migrate along the medial migratory pathway in gnathostomes was the first step in the modification of the gnathostome body plan away from their agnathan forerunners.

In the axolotl, the neural crest sheath around the mesoderm starts to lose its homogeneity after completion of the outside-in movement (stage 34–35). Some individual neural crest cells are found within the mesoderm from about stage 37 onward where they gradually differentiate into connective tissue components of cranial muscles as in other vertebrates (Noden, 1988; Olsson et al., 2001). By this stage, axolotl neural crest cells on the medial side of the arches condense into cartilage, for which an interaction with pharyngeal endoderm is required (Epperlein and Lehmann, 1975). The outside–inward movement therefore might function to bring neural crest cells close to signals from the endoderm and therefore is a prerequisite for the development of the visceroskeleton. Thus, the ring of neural crest around the arch mesoderm may be regarded as a developmentally and evolutionarily conserved feature and the

outside-in movement as an alternative developmental mechanism with which the colocalisation of neural crest and mesoderm can be achieved.

Conclusions

In this study, we have documented an autonomous migratory pattern of axolotl cranial neural crest cells in vitro and interactions of neural crest streams with neighboring tissue in vivo. The ease of visualization coupled with the availability of neural crest markers in this species has allowed us to uncover several novel mechanisms contributing to neural crest patterning. First, we note that neural crest cells migrating from cranial neural tubes migrate in distinct streams in vitro on a permissive substrate without adjacent tissue. Then we observed that close local appositions between the cranial epidermis and adjacent tissues (neural tube, mesoderm and endoderm) lead to the formation of channels that constrain laterally migrating neural crest cells and maintain distinct streams. Third, we experimentally show that removal of the epidermis leads to the fusion of neural crest streams, indicating a requirement for interactions between neural crest cells and at least one adjacent tissue. Fourth, we demonstrate that cranial neural crest cells—migrating initially only laterally—surround the mesodermal core in the branchial arches via an outside-in movement that has been proposed but never proven in other gnathostomes. Taken together, autonomy of initial cranial neural crest stream formation with stabilizing interactions between more advanced neural crest cell streams and neighboring tissues appear to play the predominant role in establishing the migratory pattern of cranial neural crest streams. The exact migratory pathways of neural crest cells seem to differ significantly across vertebrates, irrespective of conservative patterns of cranial neural crest streams. We suggest that these subtle differences in neural crest migration are mirrored later and provide morphological variations of vertebrate types.

Acknowledgments

We thank Tanya Moreno for the GFP mRNA, Irmin Beck for help in artwork, and Torsten Schwalm and Lewan Mtschedlischwili for technical advice. Support from NIH grant HD15527 and NASA grant NAG 2-1585 to M.B.F. and Herbert-Quandt Stiftung, SMWK, COST B-23, MSMT grant 1311004 and a NATO Science Fellowships Programme to R.C.

References

Alfandari, D., Cousin, H., Gaultier, A., Smith, K., White, J.M., Darribere, T., DeSimone, D.W., 2001. *Xenopus* ADAM13 is a metalloprotease required for cranial neural crest-cell migration. Curr. Biol. 11, 918–930.

Anderson, C.B., Meier, S., 1981. The influence of the metameric pattern in the mesoderm on migration of cranial neural crest cells in the chick embryo. Dev. Biol. 85, 385–402.

Birgbauer, E., Sechrist, J., Bronner-Fraser, M., Fraser, S., 1995. Rhombomeric origin and rostrocaudal reassortment of neural crest cells revealed by intravital microscopy. Development 121, 935–945.

Bradley, L.C., Snape, A., Bhatt, S., Wilkinson, D.G., 1992. The structure and expression of the *Xenopus* Krox-20 gene: conserved and divergent patterns of expression in rhombomeres and neural crest. Mech. Dev. 40, 73–84.

Chai, Y., Jiang, X., Ito, Y., Bringas Jr., P., Han, J., Rowitch, D.H., Soriano, P., McMahon, A.P., Sucov, H.M., 2000. Fate of the mammalian cranial neural crest during tooth and mandibular morphogenesis. Development 127, 1671–1679.

Christensen, R.N., Weinstein, M., Tassava, R.A., 2001. Fibroblast growth factors in regenerating limbs of *Ambystoma*: cloning, semi-quantitative RT-PCR expression studies. J. Exp. Zool. 290, 529–540.

Cole, L.K., Ross, L.S., 2001. Apoptosis in the developing zebrafish embryo. Dev. Biol. 240, 123–142.

Couly, G.F., Coltey, P.M., Le Douarin, N.M., 1993. The triple origin of skull in higher vertebrates: a study in quail-chick chimeras. Development 117, 409–429.

Del Pino, E.M., Medina, A., 1998. Neural development in the marsupial frog *Gastrotheca riobambae*. Int. J. Dev. Biol. 42, 723–731.

Eickholt, B.J., Mackenzie, S.L., Graham, A., Walsch, F.S., Doherty, P., 1999. Evidence for collapin-1 functioning in the control of neural crest migration in both trunk and hindbrain regions. Development 126, 2181–2189.

Ellies, D.L., Langille, R.M., Martin, C.C., Akimenko, M.-A., Ekker, M., 1997. Specific craniofacial cartilage dysmorphogenesis coincidates with a loss of *dlx* gene expression in retinoic acid-treated zebrafish embryos. Mech. Dev. 61, 23–36.

Epperlein, H.H., Lehmann, R., 1975. The ectomesenchymal–endodermal interaction system (EEIS) of *Triturus alpestris* in tissue culture. 2. Observations on the differentiation of visceral cartilage. Differentiation 4, 159–174.

Epperlein, H.H., Meulemans, D., Bronner-Fraser, M., Steinbeisser, H., Selleck, M.A.J., 2000. Analysis of cranial neural crest migratory pathways in axolotl using cell markers and transplantation. Development 127, 2751–2761.

Essex, L.J., Mayor, R., Sargent, M.G., 1993. Expression of *Xenopus Snail* in mesoderm and prospective neural fold ectoderm. Dev. Dyn. 198, 108–122.

Falck, P., Hanken, J., Olsson, L., 2002. Cranial neural crest emergence and migration in the Mexican axolotl (*Ambystoma mexicanum*). Zoology 105, 195–202.

Farlie, P.G., Kerr, R., Thomas, P., Symes, T., Minichiello, J., Hearn, C.J., Newgreen, D., 1999. A paraxial exclusion zone creates patterned cranial neural crest cell outgrowth adjacent to rhombomeres 3 and 5. Dev. Biol. 213, 70–84.

Golding, J.P., Dixon, M., Gassmann, M., 2002. Cues from neuroepithelium and surface ectoderm maintain neural crest-free regions within cranial mesenchyme of the developing chick. Development 129, 1095–1105.

Graham, A., Heyman, I., Lumsden, A., 1993. Even-numbered rhombomeres control the apoptotic elimination of neural crest cells from odd-numbered rhombomeres in the chick hindbrain. Development 119, 233–245.

Hacker, A., Guthrie, S., 1998. A distinct developmental programme for the cranial paraxial mesoderm in the chick embryo. Development 125, 3461–3472.

Hall, B.K., Hörstadius, S., 1988. The Neural Crest. Oxford Press, Oxford.

Han, M.-J., An, J.-Y., Kim, W.-S., 2001. Expression patterns of *Fgf-8* during development and limb regeneration of the axolotl. Dev. Dyn. 220, 40–48.

Hendzel, M.J., Wei, Y., Mancini, M.A., Van Hooser, A., Ranalli, T., Brinkley, B.R., Bazett-Jones, D.P., Allis, C.D., 1997. Mitosis-specific

phosphorylation of histone H3 initiates primarily within pericentromeric heterochromatin during G2 and spreads in an ordered fashion coincident with mitotic chromosome condensation. Chromosoma 106, 348–360.
Hensey, C., Gautier, J., 1998. Programmed cell death during *Xenopus* development: a spatio-temporal analysis. Dev. Biol. 203, 36–48.
Hirata, M., Hall, B.K., 2000. Temporospatial patterns of apoptosis in chick embryos during the morphogenetic period of development. Int. J. Dev. Biol. 44, 757–768.
Holder, N., Klein, R., 1999. Eph receptors and ephrins: effectors of morphogenesis. Development 126, 2033–2044.
Horigome, N., Myojin, M., Ueki, T., Hirano, S., Aizawa, S., Kuratani, S., 1999. Development of the cephalic neural crest cells in embryos of *Lampetra japonica*, with special references to evolution of the jaw. Dev. Biol. 207, 287–308.
Jacobson, A.G., Meier, S., 1984. Morphogenesis of the head of a newt: mesodermal segments, neuromeres, and distribution of neural crest. Dev. Biol. 106, 181–193.
Jiang, X., Iseki, S., Maxson, R.E., Sucov, H.M., Morris-Kay, G.M., 2002. Tissue origin and interactions in the mammalian skull vault. Dev. Biol. 241, 106–116.
Kimmel, C.B., Miller, C.T., Cruze, G., Ullmann, B., BreMiller, R.A., Larison, K.D., Snyder, H.C., 1998. The shaping of pharyngeal cartilages during early development of the zebrafish. Dev. Biol. 203, 245–263.
Kimmel, C.B., Miller, C.T., Keynes, R.J., 2001. Neural crest patterning and the evolution of the jaw. J. Anat. 199, 105–120.
Kubota, Y., Ito, K., 2000. Chemotactic migration of mesencephalic neural crest cells in the mouse. Dev. Dyn. 217, 170–179.
Kulesa, P.M., Fraser, S.E., 2000. In ovo time-lapse analysis of chick hindbrain neural crest cell migration shows cell interactions during migration to the branchial arches. Development 127, 1161–1172.
Kuratani, S., Eichele, G., 1993. Rhombomere transplantation repatterns the segmental organization of cranial nerves and reveals cell-autonomous expression of a homeodomain protein. Development 117, 105–117.
Le Douarin, N.M., Kalcheim, C., 1999. The Neural Crest, Second ed. Cambridge Univ. Press, New York.
Linker, C., Bronner-Fraser, M., Mayor, R., 2000. Relationship between gene expression domains of *Xsnail*, *Xslug*, and *Xtwist* and cell movement in the prospective neural crest of *Xenopus*. Dev. Biol. 224, 215–225.
Lumsden, A., Krumlauf, R., 1996. Patterning the vertebrate neuraxis. Science 274, 1109–1115.
Lumsden, A.L., Sprawson, N., Graham, A., 1991. Segmental origin and migration of neural crest cells in the hindbrain region of the chick embryo. Development 113, 1281–1291.
Mayor, R., Morgan, R., Sargent, M.G., 1995. Induction of the prospective neural crest of *Xenopus*. Development 121, 767–777.
McCauley, D.W., Bronner-Fraser, M., 2003. Neural crest contributions to the lamprey head. Development 130, 2317–2327.
McGonnell, I.M., Graham, A., 2002. Trunk neural crest has skeletogenic potential. Curr. Biol. 12, 767–771.
Meier, S., Packard Jr., D.S., 1984. Morphogenesis of the cranial segments and distribution of neural crest in the embryo of the snapping turtle, *Chelydra serpentina*. Dev. Biol. 102, 309–323.
Meulemans, D., Bronner-Fraser, M., 2002. Amphioxus and lamprey AP-2 genes: implications for neural crest evolution and migration patterns. Development 129, 4953–4962.
Noden, D.M., 1988. Interactions and fates of avian craniofacial mesenchyme. Dev. Suppl. 103, 121–140.
Noden, D.M., Marcucio, R., Borycki, A.-G., Emerson Jr., C.P., 1999. Differentiation of avian craniofacial muscles: I. Patterns of early regulatory gene expression and myosin heavy chain synthesis. Dev. Dyn. 216, 96–112.
Northcutt, R.G., Brändle, K., 1995. Development of branchiomeric and lateral line nerves in the axolotl. J. Comp. Neurol. 355, 427–454.
Olsson, L., Falck, P., Lopez, K., Cobb, J., Hanken, J., 2001. Cranial neural crest cells contribute to connective tissue in cranial muscles in the anuran amphibian, *Bombina orientalis*. Dev. Biol. 237, 354–367.
Olsson, L., Moury, J.D., Carl, T.F., Håstad, O., Hanken, J., 2002. Cranial neural crest-cell migration in the direct-developing frog, *Eleutherodactylus coqui*: molecular heterogeneity within and among migratory streams. Zoology 105, 3–13.
Osumi-Yamashita, N., Ninomiya, Y., Doi, H., Eto, K., 1994. The contribution of both forebrain and midbrain crest cells to the mesenchyme in the frontonasal mass of mouse embryos. Dev. Biol. 164, 409–419.
Piotrowski, T., Nüsslein-Volhard, C., 2000. The endoderm plays an important role in patterning the segmented pharyngeal region in zebrafish (*Danio rerio*). Dev. Biol. 225, 339–356.
Riou, J.-F., Delarue, M., Méndez, A.P., Boucaut, J.-C., 1998. Role of fibroblast growth factor during early midbrain development in *Xenopus*. Mech. Dev. 78, 3–15.
Robinson, V., Smith, A., Flenniken, A.M., Wilkinson, D.G., 1997. Roles of Eph receptors and ephrins in neural crest pathfinding. Cell Tissue Res. 290, 265–274.
Sadaghiani, B., Thiébaud, C., 1987. Neural crest development in the *Xenopus laevis* embryo, studied by interspecific transplantation and scanning electron microscopy. Dev. Biol. 124, 91–110.
Sadaghiani, B., Vielkind, J.R., 1989. Neural crest development in *Xiphophorus* fishes: scanning electron and light microscopy studies. Development 105, 487–504.
Saka, Y., Smith, J.C., 2001. Spatial and temporal patterns of cell division during early *Xenopus* embryogenesis. Dev. Biol. 229, 307–318.
Saldivar, J.R., Krull, C.E., Krumlauf, R., Ariza-McNaughton, L., Bronner-Fraser, M., 1996. Rhombomere of origin determines autonomous versus environmentally regulated expression of *Hoxa3* in the avian embryo. Development 122, 895–904.
Schilling, T.F., Kimmel, C.B., 1994. Segment and cell type lineage restrictions during pharyngeal arch development in the zebrafish embryo. Development 120, 483–494.
Schneider, S., Steinbeisser, H., Warga, R.M., Hausen, P., 1996. Beta-catenin translocation into nuclei demarcates the dorsalizing centers in frog and fish embryos. Mech. Dev. 57, 191–198.
Sechrist, J., Serbedzija, G.N., Scherson, N., Fraser, S.E., Bronner-Fraser, M., 1993. Segmental migration of the hindbrain neural crest does not arise from its segmental generation. Development 118, 691–703.
Serbedzija, G.N., Bronner-Fraser, M., Fraser, S.E., 1989. A vital dye analysis of the timing and pathways of avian trunk neural crest cell migration. Development 106, 809–816.
Serbedzija, G.N., Bronner-Fraser, M., Fraser, S.E., 1992. Vital dye analysis of cranial neural crest cell migration in the mouse embryo. Development 116, 297–307.
Shen, H., Wilke, T., Ashique, A.M., Narvey, M., Zerucha, T., Savino, E., Williams, T., Richman, J.M., 1997. Chicken transcription factor AP-2: cloning, expression and its role in outgrowth of facial prominences and limb buds. Dev. Biol. 188, 248–266.
Shimeld, S.M., Holland, P.W.H., 2000. Vertebrate innovations. Proc. Natl. Acad. Sci. U. S. A. 97, 4449–4452.
Smith, A., Graham, A., 2001. Restricting Bmp-4 mediated apoptosis in hindbrain neural crest. Dev. Dyn. 220, 276–283.
Smith, A., Robinson, V., Patel, K., Wilkinson, D.G., 1997. The EphA4 and EphB1 receptor tyrosine kinases and ephrin-B2 ligand regulate targeted migration of branchial neural crest cells. Curr. Biol. 7, 561–570.
Tan, S.S., Morris-Kay, G.M., 1986. Analysis of cranial neural crest cell migration and early fates in postimplantation rat chimaeras. J. Embryol. Exp. Morphol. 98, 21–58.
Trainor, P.A., Krumlauf, R., 2000a. Plasticity in mouse neural crest cells reveals a new patterning role for cranial mesoderm. Nat. Cell Biol. 2, 96–102.
Trainor, P.A., Krumlauf, R., 2000b. Patterning the cranial neural crest: hindbrain segmentation and *Hox* gene plasticity. Nat. Rev. Neurosci. 1, 116–124.
Trainor, P.A., Tam, P.P.L., 1995. Cranial paraxial mesoderm and neural

crest cells of the mouse embryo: co-distribution in the craniofacial mesenchyme but distinct segregation in branchial arches. Development 121, 2569–2582.

Trainor, P.A., Sobieszczuk, D., Wilkinson, D., Krumlauf, R., 2002. Signalling between the hindbrain and paraxial tissues dictates neural crest migration pathways. Development 129, 433–442.

Trumpp, A., Depew, M.J., Rubenstein, J.L.R., Bishop, J.M., Martin, G.R., 1999. Cre-mediated gene inactivation demonstrates that FGF8 is required for cell survival and patterning of the first branchial arch. Genes Dev. 13, 3136–3148.

Veitch, E., Begbie, J., Schilling, T.F., Smith, M.M., Graham, A., 1999. Pharyngeal arch patterning in the absence of neural crest. Curr. Biol. 9, 1481–1484.

Zou, H., Niswander, L., 1996. Requirement for BMP signaling in interdigital apoptosis and scale formation. Science 272 (5262), 738–741.